

PAPER • OPEN ACCESS

Finite Element Analysis of Wave-Front Aberrations of Medium and High Myopia with Different CCT after Small Incision Lenticule Extraction (SMILE)

To cite this article: Tianzi Jin and Lihua Fang 2022 *J. Phys.: Conf. Ser.* **2383** 012104

View the [article online](#) for updates and enhancements.

You may also like

- [Importance of Axial Length Measurement in Routine Clinical Practice](#)
Irene Joseph, Reetu Malhotra and Anupama Prasan Rao
- [A scalable and deformable stylized model of the adult human eye for radiation dose assessment](#)
Daniel El Basha, Takuya Furuta, Siva S R Iyer et al.
- [Dioptres for a myopic eye from a photo](#)
Michael J Ruiz



ECS
The
Electrochemical
Society
Advancing solid state &
electrochemical science & technology

DISCOVER
how sustainability
intersects with
electrochemistry & solid
state science research

Finite Element Analysis of Wave-Front Aberrations of Medium and High Myopia with Different CCT after Small Incision Lenticule Extraction (SMILE)

Tianzi Jin^{1a*}, Lihua Fang^{1b*}

¹Key Laboratory of Nondestructive Test (Ministry of Education), Nanchang Hangkong University, Nanchang, 330063, China

^{a*}wsxxjtz@163.com, ^{b*}fanglh71@126.com

Abstract—In this study, the wave-front aberrations of medium and high myopia with different CCT after SMILE were studied by the finite element method. Then, the various trend of wave-front aberrations with clinical significance was obtained. When CCT was the same, the wave-front aberrations of myopia with different diopters were different. When CCT increased, the variations of wave-front aberrations of myopia with different diopters were different. However, regardless of the degree of myopia, the variations of defocus and primary spherical aberration were the most obvious. The larger the CCT, the smaller the absolute values of defocus and primary spherical aberration.

1. Introduction

In SMILE, the laser is used to cut the cornea. Then, the lens tissue is separated to achieve the correcting vision^[1,2]. The thickness of the lens tissue depends on the actual condition of the eyes, such as SPH, CYL, EOZ, and so on. In the normal conditions of the eyes, the higher the degree of SPH, the thicker the lens tissue to be cut. In addition, the cornea with too small CCT cannot be cut to obtain too thick lens tissue. Otherwise, the remaining cornea will be too thin. It affects postoperative recovery and visual imaging quality. However, within the range of safe cutting thickness, myopia with different CCT leads to different wave-front aberrations. The various trend needs to be further studied and analyzed.

Finite element analysis is a perfect analysis method. By this method, the complex region is divided into several simple sub-regions. Then, the sub-regions are solved to produce stable solutions. Finite element analysis is also used in ophthalmology: Grytz R et al. used the finite element eye models to study complex anisotropic materials^[3]; Vivek Suganthan R et al. conducted finite element analysis on intraocular pressure of human eyes^[4]; Osmer J et al. used adaptive finite element eye models to study intraocular pressure^[5].

In this study, the postoperative human eye finite element models with different CCT were established. Then, the wave-front aberrations of medium and high myopia were studied. Finally, the various trend of the wave-front aberrations with clinical significance was obtained.

2. Methods

2.1 Human eye finite element model

The steps included establishing the 3D finite element models of personalized human eyes, defining



material parameters, setting intraocular pressure and other boundary conditions, and selecting meshing. After these steps, the finite element method was used to analyze the wave-front aberrations caused by the displacements.

The clinical data of myopia before and after SMILE was obtained from the eye hospital. Based on the data, the six kinds of personalized preoperative and postoperative finite element models were established, respectively.

In this study, the models were divided into three groups by the degree of SPH: Group One (-4.75 D and -5 D), Group Two (-6.5 D), and Group Three (-8 D). It was worth mentioning that the degree of CYL of each myopia was small (within -0.5 D). In addition, the CCT studied included 520 μm , 550 μm , and 580 μm . The maximum difference was 60 μm , and it made the comparison of results more obvious.

One of the postoperative finite element models of the personalized human eyes as shown in Figure 1. The surgical simulation data of six kinds of personalized models is shown in Table 1.

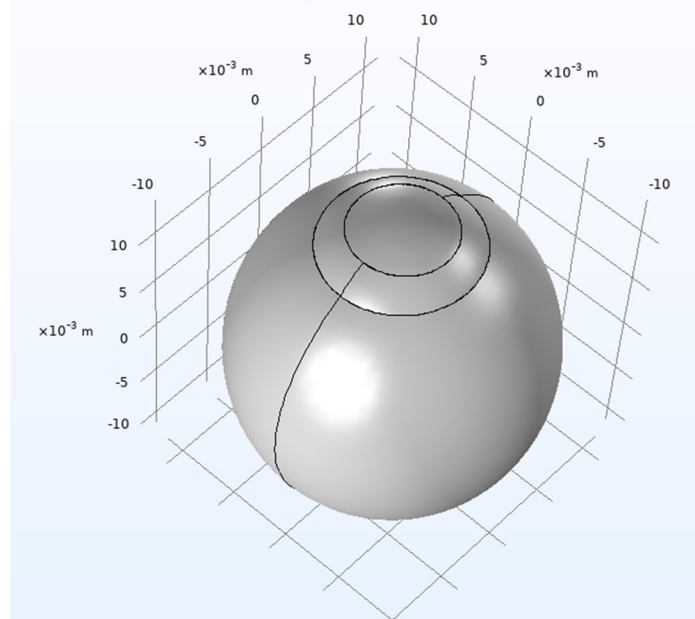


Fig.1 the postoperative finite element model of the personalized human eye

Table 1 the surgical simulation data of six kinds of personalized models

Group	Case	Lens Thickness/ μm	Cap Thickness/ μm	SPH/D	CYL/D
Group One	Case One	107	120	-5	-0.5
	Case Two	103	120	-4.75	-0.5
Group Two	Case Three	136	120	-6.5	-0.25
	Case Four	136	120	-6.5	-0.25
Group Three	Case Five	160	110	-8	-0.25
	Case Six	160	110	-8	-0.25

2.2 Material parameters

For the human cornea, the Bowman's layer has the strongest biomechanical strength. Moreover, the biomechanical strength of the front corneal stromal layer is better than that of the rear corneal stromal layer^[1]. This study was to control the distribution of material parameters by programming. It improved the simulation degree of the finite element models of human eyes. More specifically, Young's modulus of the cornea changed regularly with the depth of the cornea. It decreased from 1.6MPa in the front corneal stromal layer to 0.8MPa in the rear^[6,7].

In addition, the ratio of Young's modulus of the cornea and the sclera is fixed^[8]. This study kept the ratio unchanged at 1:3. It is worth noting that physical conditions such as intraocular pressure must be considered in human eye simulation. In this study, the intraocular pressure was 15mmHg^[8,9].

The distribution of corneal Young's modulus through the XZ plane as shown in Figure 2.

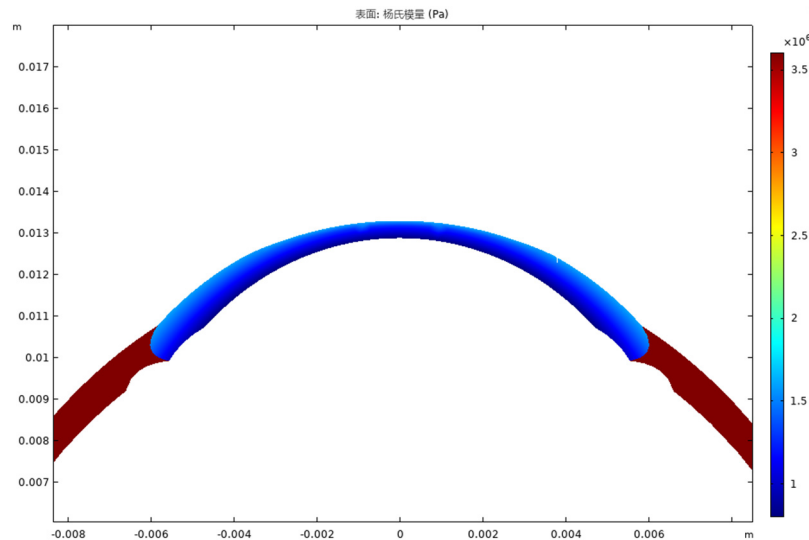
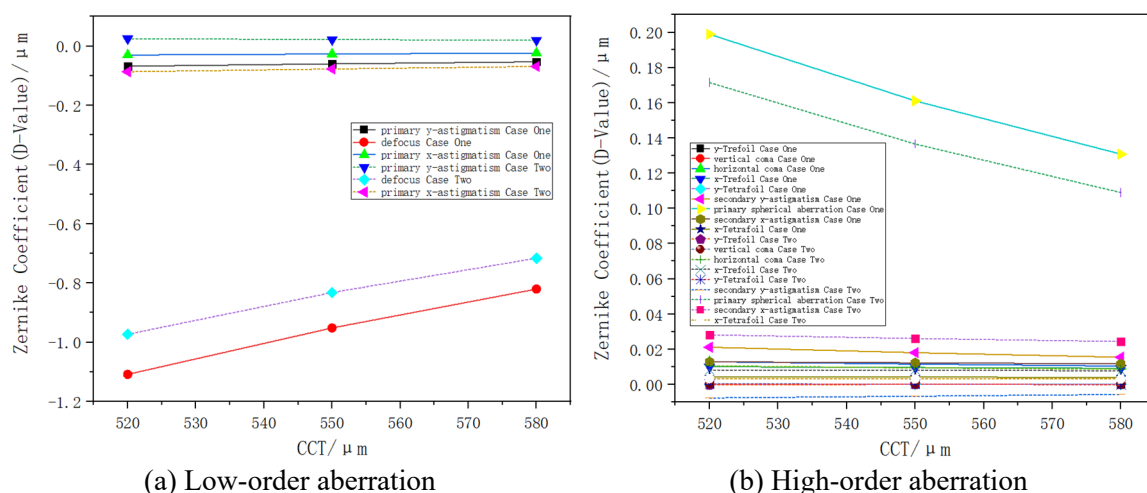


Fig.2 the distribution of corneal Young's modulus

2.3 Biomechanical analysis

The wave-front aberrations caused by the displacements of the anterior and posterior corneal surfaces are partially compensated for each other. In addition, the values of the two differ by an order of magnitude^[8]. This study aimed to study the influence of different CCT on wave-front aberrations. The focus was on the various trend rather than the specific values. Therefore, only wave-front aberrations caused by the displacement of the anterior corneal surface were analyzed in this study.

3. Result



(a) Low-order aberration

(b) High-order aberration

Fig.3 Aberrations caused by the displacement of the anterior corneal surface of Group One

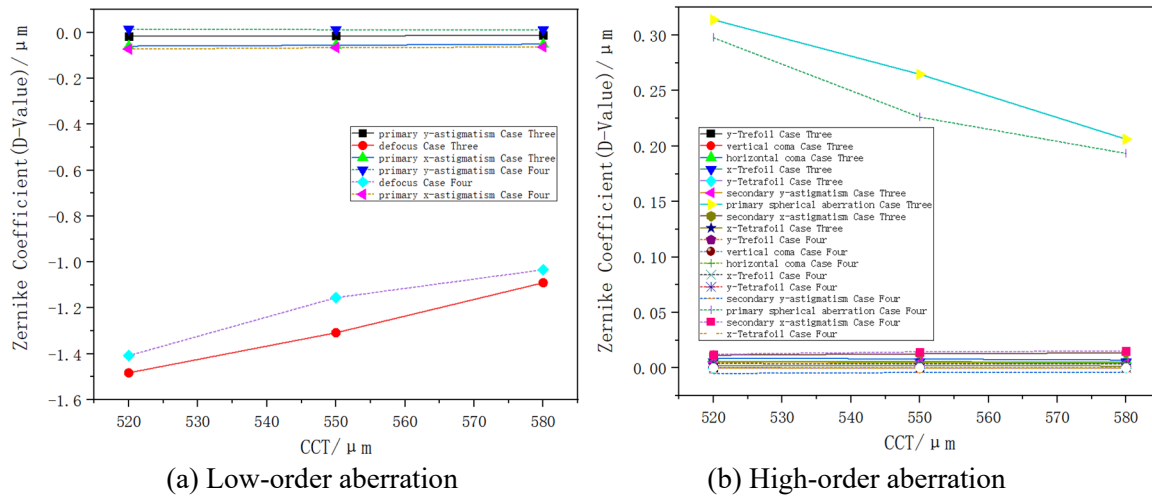


Fig.4 Aberrations caused by the displacement of the anterior corneal surface of Group Two

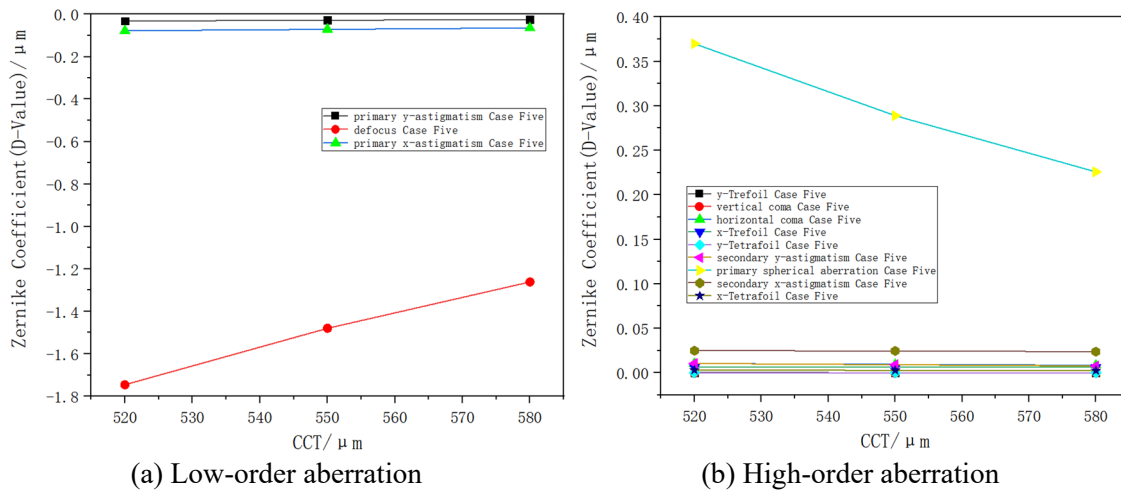


Fig.5 Aberrations caused by the displacement of the anterior corneal surface of Group Three

Regardless of the degree of myopia, the larger the CCT, the smaller the absolute values of defocus and primary spherical aberration. In contrast, the values of other low-order and high-order aberrations were small and showed little change. Therefore, the CCT had the most significant influence on the defocus and primary spherical aberration after SMILE.

When CCT increased, the various trend of wave-front aberrations of myopia with different diopters was the same, but the variations were different. When CCT increased from 520 μm to 580 μm, the absolute values of defocus of Group One, Group Two, and Group Three decreased by 0.2879 μm and 0.2568 μm, 0.3926 μm and 0.3742 μm, and 0.4845 μm, respectively. While, the absolute values of primary spherical aberration decreased by 0.0681 μm and 0.0625 μm, 0.1077 μm and 0.1042 μm, and 0.1440 μm, respectively.

In addition, at the same CCT, the values of the wave-front aberrations of eyeballs with different myopia degrees were different. For example, when CCT was 550 μm, the values of defocus of Group One, Group Two, and Group Three were -0.9517 μm and -0.8322 μm, -1.3078 μm and -1.1553 μm, and -1.4802 μm, respectively. While, those of primary spherical aberration were 0.1611 μm and 0.1365 μm, 0.2648 μm and 0.2261 μm, and 0.2890 μm, respectively. The biomechanical response of the cornea might be affected by the lens thickness, the cap thickness, or the astigmatism degree in different diopter groups. Thus, the numerical difference between aberrations was resulted.

4. Conclusion

When CCT was the same, the wave-front aberrations of myopia with different diopters were different. When CCT increased, the variations of wave-front aberrations of myopia with different diopters were different. However, regardless of the degree of myopia, the variations of defocus and primary spherical aberration were the most obvious. The larger the CCT, the smaller the absolute values of defocus and primary spherical aberration.

These conclusions had specific clinical guiding significance. When myopic eyes undergo SMILE, the lens thickness should be considered in combination with the CCT and refractive states. Because different CCT and refractive conditions will lead to different corrective effects. The postoperative corrective effects of SMILE can be comprehensively studied by using the finite element method combined with the CAP thickness and CYL.

Acknowledgments

This study was supported by the Natural National Science Foundation of China (NSFC) (62165010 & 81873684), The National Key Research and Development Program of China (2018YFE0115700)

References

- [1] Yang Dandan, Yin He. Study on the early changes of posterior corneal elevation in myopia patients after small incision lenticule extraction [J]. *Journal of Clinical Ophthalmology*, 2020,28(6):518-521.
- [2] Wu Y, Huang Z. Comparison of early visual quality in patients with moderate myopia using different optical zones in small incision lenticule extraction (SMILE) [J]. *BMC Ophthalmology*, 2021, 21(1): 1-8.
- [3] Grytz R, Krishnan K, Whitley R, et al. A mesh-free approach to incorporate complex anisotropic and heterogeneous material properties into eye-specific finite element models [J]. *Computer methods in applied mechanics and engineering*, 2020, 358: 112654.
- [4] Vivek Suganthan R, Meenatchi Sundaram S, Ramesh S V, et al. Finite element analysis of the human eye for a range of intraocular pressure [M] // *Advances in Control Instrumentation Systems*. Springer, Singapore, 2020: 173-181.
- [5] Osmers J, Kaiser N, Sorg M, et al. Adaptive finite element eye model for the compensation of biometric influences on acoustic tonometry [J]. *Computer Methods and Programs in Biomedicine*, 2021, 200(10108):105930.
- [6] Labate C, Lombardo M, De Santo M P, et al. Multiscale investigation of the depth-dependent mechanical anisotropy of the human corneal stroma [J]. *Investigative ophthalmology & visual science*, 2015, 56(6): 4053-4060.
- [7] Mikula E R, Jester J V, Juhasz T. Measurement of an elasticity map in the human cornea [J]. *Investigative ophthalmology & visual science*, 2016, 57(7): 3282-3286.
- [8] Fang L, Ma W, Wang Y, et al. Theoretical analysis of wave-front aberrations induced from conventional laser refractive surgery in a biomechanical finite element model [J]. *Investigative Ophthalmology & Visual Science*, 2020, 61(5): 34-34.
- [9] Chen Xiuguo, Shen Min, Wang Yan, et al. Finite Element Analysis of Corneal Deformation and Stress after LASIK [J]. *Chinese Journal Of Optometry Ophthalmology And Visual Science*, 2019, 21(2):7.